Assessing Native and Non-native Conformational States of a Protein by Methylene Carbene Labeling: The Case of *Bacillus licheniformis* β-Lactamase

Daniela B. Ureta, Patricio O. Craig,‡ Gabriela E. Gómez, and José M. Delfino*

Departamento de Química Biológica-IQUIFIB (UBA-CONICET), Facultad de Farmacia y Bioquímica, Universidad de Buenos Aires, Junín 956, C1113AAD, Buenos Aires, Argentina

Received June 29, 2007; Revised Manuscript Received October 10, 2007

ABSTRACT: Much knowledge of protein folding can be derived from the examination of the nature and size of solvent-exposed surfaces along conformational transitions. We exploit here a general photochemical modification with methylene carbene of the accessible surface area (ASA) of the polypeptide chain. Labeling of *Bacillus licheniformis* β-lactamase (BL-βL) with 1 mM ^{3}H-diazirine yielded 8.3×10^{-3} mol CH_2/mol protein, in agreement with the prediction for an unspecific surface labeling phenomenon. The unfolded state U in 7 M urea was labeled 60% more than the native state N. This result lies well below the increment of ASA expected from theoretical estimates and points to the presence of residual organization in state U and/or of cavities or crevices favoring the partition of the reagent in state N. A partially folded state I was demonstrated from two sequential transitions occurring at 1.5−3.0 M and 3.5−6.5 M urea. This technique shows a close correlation with optical probes most sensitive to changes in tertiary structure, a statement supported by the fact that the largest change occurs along the N−I portion of the N−I−U transition and along the acid pH-induced N−A transition. In the latter case, state A is labeled 70% more than state N, an increment consistent with the loosening of tight interactions in the core of the protein. Fragmentation of labeled BL-βL into peptides provides a sequential map of solvent accessibility. Thus, amino acid residues pertaining to the Ω-loop and to helices α5 and α6 line the major cavity of the protein, that is big enough to lodge the diazirine reagent. Methylene labeling, by introducing an original (and perhaps unique) experimental measurement of ASA, enlightens subtle aspects of complex transitions and makes possible a comparative structural characterization of the native as well as non-native states.

Proteins represent essential building blocks behind cell structure and the engines supporting every metabolic reaction. The close relationship existing between the detailed conformation and function of proteins substantiates the current emphasis on their structural studies. In this context, the characterization of the native state, as well as the unfolded and intermediate states, constitutes an important issue in protein science. The native state is marginally stable with respect to alternative conformations. Thus, it can be readily perturbed by subtle changes of the physicochemical environment. At the other end, the unfolded ensemble of states can be stabilized under strong denaturing conditions and exhibits open and highly flexible conformations characterized by extensive exposure of the polypeptide chain to the aqueous solvent. Finally, under milder denaturing conditions, intermediate states can indeed be populated (*1*). One typical example of the latter is the so-called molten globule state (*2*, *3*). Among its distinctive features, one can mention that it adopts a globular but less compact conformation than the native state, giving rise to a slightly expanded form endowed with substantial secondary structure but lacking specific tertiary contacts. Thus, the increased mobility of hydrophobic side chains in the semiliquid core facilitates the access of the aqueous solvent to otherwise excluded regions in the native state. The importance of studying intermediate states in equilibrium cannot be underestimated because they have been postulated to share similar features to late kinetic intermediates detected along folding pathways, thus shedding light on the general process of protein folding.

The knowledge of intermediate and unfolded states has been hampered by the lack of appropriate high-resolution techniques to address their conformation. Extensive fluctuations of the polypeptide chain in a very short time scale hinder the useful application of techniques such as X-ray crystallography or NMR. In this context, optical methods (CD, fluorescence, light scattering), chemical techniques (H/D exchange, chemical modification of side chains of amino acids), and size-exclusion chromatography, coupled to defined alteration of the amino acid sequence (site-directed mutagenesis, truncations, construction of chimaeras, etc.) have been used with profit to address specific structural aspects. Although unable to provide a thorough picture, these

† D.B.U. was a recipient of a graduate student fellowship from the FOMEC program. G.E.G. was a recipient of a graduate student fellowship from the University of Buenos Aires (UBA) and is currently an Estenssoro fellow from the YPF Foundation. P.O.C. and J.M.D. are career investigators of CONICET. This research has been supported by grants to J.M.D. from Universidad de Buenos Aires (UBA), the Consejo Nacional de Investigaciones Científicas y Técnicas (CONICET), and the Agencia Nacional de Promoción Científica y Tecnológica (ANPCyT).

* Author to whom correspondence should be addressed. E-mail: delfino@qb.ffyb.uba.ar, tel: 54 11 4964 8291, extension 116, fax: 54 11 4962 5457.

‡ Current address: Fundación Instituto Leloir, Av. Patricias Argentinas 435, C1405BWE, Buenos Aires, Argentina.

10.1021/bi7012867 CCC: $37.00
Published on Web 11/17/2007

techniques are very valuable tools to gain insights on structure because they can be adapted to the various timescales of the folding process (for general references see refs 4−7).

In regard to the thermodynamics of folding, minimization of the accessible surface area (ASA[1]) associated to the hydrophobic side chains and the amide groups of the peptide bonds has been generally recognized as an important structural parameter (*8*−*10*). A fundamental issue worth investigating is to be able to describe the nature as well as to measure the extension of the ASA at each stage of the process. Unfortunately, there is hardly any technique appropriate to address a direct experimental measurement of ASA. In this regard, the chemical reactivity of a given functional group present on an amino acid side chain against a set of reagents of different nature can provide a description of the environment around this group, thus making it possible to infer solvent accessibility to this point region. However, drawbacks of the selective chemical modification techniques are to strictly control the extent of modification, the occurrence of side reactions, and the frequent induction of conformational changes and to be constrained to alter a single or a few chemical functionalities (*11*). On the other hand, proton−deuteron (H/D) exchange has been widely applied in protein folding because it addresses the accessibility of exchangeable protons along the polypeptide chain without introducing hardly any modification in chemical nature. Although one can derive a landscape of solvent accessibility with this technique, it is noteworthy that data is intrinsically limited to amide protons belonging to the backbone chain, therefore becoming strongly dependent on secondary structure integrity. Besides, one main drawback arises from the labile nature of the label, a factor that greatly restricts further analytical processing of the sample. By contrast, a reagent aimed to act as a *general probe* should define the protein surface *independently* of its chemical nature. From a chemical standpoint, successful modification of the inert surface provided by the hydrophobic side chains poses an absolute requirement for a free radical, or a photogenerated nitrene or carbene. Along these lines, there have been recent developments toward the general labeling of proteins. Among these, one can mention the use of the hydroxyl radical chemistry (•OH) (*12*−*18*), and another technique, put forward by Richards et al. (*19*) and developed in our own laboratory, takes advantage of the modification of the polypeptide chain with singlet methylene ($:CH_2$) (*20*−*22*).

The extreme reactivity of methylene makes it an ideal reagent to achieve nonselective chemical modification of proteins. Unlike other radical species that give rise to chain reactions, methylene inserts readily into any X−H bond yielding defined and stable methylated products. Diazirine (DZN) fulfills all the requirements to become the source reagent of methylene. In this regard, trifluoromethylphenyl-substituted diazirines have been widely used in hydrophobic photolabeling of membrane proteins (e.g., see refs *23*, *24*, and references cited therein). However, to achieve solvent mimicry, one relies on the fact that unsubstituted DZN is comparable in size to the water molecule, so DZN is expected to probe the same surface as the aqueous solvent. In addition, DZN is a chemically inert gas at room temperature, and only after photolysis at the correct wavelength (∼320 nm) does it generate the reactive methylene species.

In this work we take advantage of the DZN labeling method, aided by the traceability provided by a ^3H label in the molecule, to address the study of the native state, intermediate species along the folding pathway, and the unfolded ensemble of states in the paradigm protein system represented by *B. licheniformis* β-lactamase (BL-β*L*). To this end, we employed the exo-small variant of this enzyme isolated from bacterial cultures (*5*). In addition to the wealth of knowledge available on this enzyme, including a high-resolution structure derived from X-ray crystallography (*26*, *27*), this protein constitutes an alternative model to α-lactalbumin, that was studied earlier in our laboratory, both because of its different folding motif and of its larger size. Most relevant to the goal of this work, intermediate states of BL-β*L* can be stabilized with the aid of denaturing agents, at acidic pH or after the addition of salts (*28*), rendering them amenable to study by DZN labeling. In this framework, we address here for the first time a comparative analysis of ASA, as inferred by the extent of modification with methylene, among differently folded states of the single-domain protein BL-β*L*.

EXPERIMENTAL PROCEDURES

Materials. ^3H-Formaldehyde (1−5 mCi, 90.0 mCi/mmol) was purchased from New England Nuclear, formaldehyde, 37% (w/v), was from E. Merck, and formamide, urea, and guanidine hydrochloride were from Sigma Chemical Co. Urea was recrystallized from ethanol before use. TPCK trypsin was from Worthington. Acetonitrile from E. Merck and trifluoroacetic acid (TFA) from Riedel de Haën were of HPLC grade. All other reagents and chemicals used were of analytical grade.

BL-β*L* and its CNBr and tryptic peptides were separated on an ÄKTA purifier (Amersham Pharmacia Biotech) and Rainin Dynamax FPLC/HPLC systems. UV measurements were carried out on a Jasco 7850 spectrophotometer.

Circular Dichroism. Spectra were recorded on Jasco J-20 and Jasco J-810 spectropolarimeters, using quartz cylindrical cuvettes of 1 or 10 mm path lengths for the far (200−250 nm) and near (250−310 nm) UV regions, respectively. In every case, five consecutive spectra were recorded and averaged to reduce the signal-to-noise ratio. Data were converted to molar ellipticity $[\theta]_M$ (in units of deg cm^2 dmol^{-1}) using a mean residue weight value for BL-β*L* of 110.49 g/mol.

Fluorescence Spectroscopy. Measurements were carried out with an Aminco Bowman Series II spectrofluorometer, using a cuvette of 0.4 cm path length. For intrinsic tryptophan fluorescence measurements, we used excitation and emission bandwidths of 4 nm and an excitation wavelength of 290 nm to selectively excite W residues present in the protein, and the emission was collected in the range 300−450 nm. For fluorescence of the extrinsic probe ANS measurements,

[1] Abbreviations: DZN, diazirine; ^3H-DZN, tritiated derivative of diazirine; $:CH_2$, methylene carbene; ASA, accessible surface area; BL-β*L*, *Bacillus licheniformis* β-lactamase (exo-small variant); α-LA, bovine α lactalbumin; HEWL, hen egg white lysozyme; N, native state; U, unfolded state; I, partially folded state; A, acid-stabilized molten globule-like state; CD, circular dichroism; ANS, 1-anilino-8-naphthalenesulfonic acid; RP-HPLC, reversed-phase high-performance liquid chromatography.

we used excitation and emission bandwidths of 4 nm and an excitation wavelength of 380 nm, and the emission was collected in the range 450−550 nm.

Expression, Purification, and Characterization of BL-βL. BL-βL was expressed in *E. coli* BL21 (DE3) and isolated from the bacterial cultures as described by Frate et al. (*25*). Transformed cells of this *E. coli* strain were produced by Dr. Anthony Fink's laboratory (University of California at Santa Cruz) and were a gift to our laboratory of Dr. Mario Ermácora (Universidad de Quilmes, Buenos Aires, Argentina). The protein was purified by a method described previously (*29*). Its functionality was monitored by enzymatic activity measurements according to Jansson (*30*), using benzylpenicillin (penicillin G) as substrate and measuring the hydrolysis of the β-lactam ring by the decrease in the absorption at 240 nm. The identity and purity of the expressed protein were assessed through the following assays: SDS-PAGE electrophoresis (*31*), reversed phase HPLC, UV absorption, and CD spectra. The concentration of exo-small *B. licheniformis* β-lactamase (BL-βL) was determined by its UV absorption at 280 nm, using a molar extinction coefficient of 23,430 M^{-1} cm^{-1} (*32*).

Synthesis of DZN. ^{3}H-DZN was synthesized and purified in our laboratory by following the method described by Craig et al. (*20*). ^{3}H-DZN concentration in aqueous solution was estimated both by measuring (i) the absorbance of the dissolved gas at 320 nm using an extinction coefficient of $\epsilon_{320} = 180$ M^{-1} cm^{-1} (*20*) and (ii) the concentration of radioactivity of the solution after complete photolysis of ^{3}H-DZN to ^{3}H-methanol had taken place.

Photolabeling of BL-βL. ^{3}H-DZN (0.2−1 mCi/mmol) was dissolved in samples of BL-βL (30 μM), with (i) 20 mM sodium phosphates buffer, pH 7.4, in the presence of different urea concentrations (0−7 M), (ii) 90 mM AGT buffer (30 mM acetate, 30 mM glycine, 30 mM Tris), pH adjusted with HCl to a given value in the range 2.0−7.0, or (iii) 90 mM AGT buffer, pH 2.0 in the presence of different urea concentrations (0−7 M), depending on the conformational transition under study: N−U, N−A, or A−U, respectively. Each sample was placed in a quartz cuvette (4 mL) of 1 cm path length and capped with a Teflon stopper. The buffers used were degassed in advance and kept under an inert atmosphere of nitrogen gas before use. Photolysis was carried out using a UV light source (Philips HPA 1000 Halogen/Hg lamp) placed at 12 cm from the samples. Light was filtered from the emission below 300 nm (with Oriel 59044 long-pass filter) to prevent photolytic damage to protein chromophores. The cuvettes were immersed in a water bath thermostated at 20 °C, so that even at the high luminic flux used, no heating occurred. Typically, UV irradiation was extended for 45 min, a time that corresponds to approximately four-half-lives of the reagent in our photolysis setup ($t_{1/2} = 10.3$ min).

After photolysis, the routine workup procedure consists of an unfolding step of the protein in 8 M urea, followed by dialysis against 0.07 mM Na_2CO_3 (pH 7.5−8.0) and freeze drying. Finally, the samples were dissolved in 6 M guanidine hydrochloride in 0.05% TFA and separated from any remaining radioactive impurity by reversed phase HPLC on a C4 column (Vydac 214TP510, 10 mm × 250 mm), developed with a linear gradient of acetonitrile:water (0 to 80% in 80 min) in 0.05% TFA at a 3.0 mL/min flow rate.

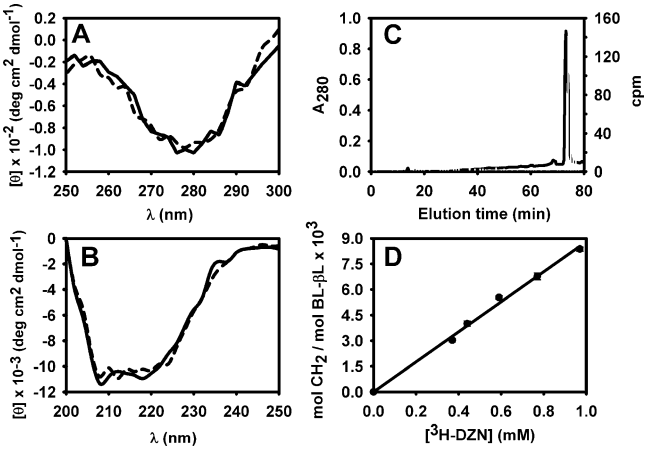

FIGURE 1: Near (A) and far (B) ultraviolet−circular dichroism (UV−CD) spectra of a 25 μM BL-βL solution in 20 mM sodium phosphate buffer, pH 7.4, before (solid lines) and after (dashed lines) the addition of DZN (3 mM final concentration) and UV irradiation for 40 min. (C) Separation of BL-βL labeled with ^{3}H-DZN by RP-HPLC on a C4 column. After the cleanup procedure (see Experimental Procedures), the labeled protein sample was chromatographed through an HPLC C4 column eluted with a linear gradient of acetonitrile:water (0 to 80% in 80 min) in 0.05% TFA at a 1.0 mL/min flow rate. Elution was monitored by both ultraviolet absorption at 280 nm (solid line) and by the measurement of the radioactivity associated to each collected fraction (gray bars). (D) Labeling of BL-βL as a function of ^{3}H-DZN concentration. The photolyzed samples contained BL-βL (35 μM) dissolved in 20 mM sodium phosphate buffer, pH 7.4. The extent of methylene carbene incorporation into the protein sample was expressed as the average number of moles of CH_2 per mole of protein.

The elution was monitored by UV absorption at 280 nm, and the protein was collected manually. For analytical purposes (see Figure 1C), samples were run on a smaller C4 column (Vydac 214TP54, 4.6 mm × 250 mm) with an identical gradient at a 1.0 mL/min flow rate. Samples cleaned in this fashion were freeze-dried to remove HPLC solvents and redissolved in 20 mM sodium phosphates buffer, pH 7.4, before the radioactivity was measured on a Pharmacia 1214 Rackbeta liquid scintillation counter. The extent of ^{3}H-methylene carbene incorporation into BL-βL was expressed as the average number of moles of CH_2 per mol of protein, as estimated by the radioactivity measured on a sample of known protein concentration, by taking into account the specific radioactivity of the reagent.

Fragmentation of BL-βL into Peptides. After the cleanup procedure described before, samples of BL-βL labeled with ^{3}H-methylene under native (20 mM sodium phosphates buffer, pH 7.4) or denaturing conditions (in the presence of 8 M urea) were cleaved with CNBr following the procedures previously described by Kamp (*33*) and Fontana and Gross (*34*). After the separation of the resultant peptides (see section below), in some instances, a complete tryptic subdigestion of fragments was achieved with TPCK trypsin in 0.1 M NH_4CO_3H, pH 8.0, after 12−18 h at 37 °C, using a 2% (w/ w) enzyme/substrate ratio, following the method described by Wilkinson (*35*).

Peptide Mapping. Separation of mixtures of peptides obtained by CNBr treatment of BL-βL was carried out by RP-HPLC on a C4 column (Vydac 214TP510, 10 mm × 250 mm), using a linear gradient of acetonitrile:water (0 to 60% in 90 min) in 0.05% TFA at a 3.0 mL/min flow rate. For analytical purposes a smaller amount of the peptide

mixtures was sampled (inset to Figure 5). The elution was monitored by UV absorption at 215 nm, and fractions were collected and subsequently identified as described below.

Tryptic peptides obtained from subdigestion of CNBr fragments were separated by size exclusion chromatography on a Superdex Peptide HR 10/30 column (Amersham Pharmacia Biotech) developed with buffer 40 mM Tris/HCl, 4 M urea, pH 7.4, at a flow rate of 0.4 mL/min. Elution was monitored by UV absorption at 215 and 280 nm, and peaks were collected manually.

Peptide identification was achieved by (i) amino acid analysis on an Applied Biosystems 420 A amino acid analyzer, (ii) Edman sequencing (*36*) where every sample was subjected to 3−5 cycles, or (iii) electrospray MS on a Thermo Finnigan LCQ Duo-ion trap mass spectrometer.

Molecular Modeling. Calculations of the ASA of BL-βL and its peptides in the native state (ASA N) were based on the crystallographic structure available for this protein (pdb code: 4blm: *24*) with the program MacroModel (*37*) using a probe radius of 1.4 Å. Considering DZN as an idealized sphere of radius 2.1 Å did not produce significant differences in the estimates of ASA. The interactive module of this program was used for constructing the protein and its CNBr peptides in extended chain conformations with the aim of calculating ASA extended. Additional ASA estimates of the unfolded protein and its peptides were obtained through a web resource (http://roselab.jhu.edu/utils/unfolded.html: (*38*, *39*) that makes use of models that bracket the surface area of the unfolded state between limiting extremes (ASA max and ASA min). The analysis of cavities present in native BL-βL was based on coordinates of structure 4blm devoid of water molecules, and performed with the program MSP (*40*) using a probe radius of 1.4 Å. Figure 6 was rendered with the program Grasp (*41*). MacroModel, MSP, and Grasp were run on SGI workstations (Indigo R4000 XS24Z and O2 R10000).

RESULTS

Photoreaction of ^{3}H-DZN with BL-βL. The unspecific ^{3}H-methylene labeling of the polypeptide chain provides a tool useful for shedding light on structural features of the native as well as non-native states. In this work we address the general applicability of this method to study the conformational transitions experienced by *Bacillus licheniformis* β-lactamase (exo-small variant: BL-βL).

A critical control that enables one to extract useful structural information from this labeling reaction consists of demonstrating that exposure to the ^{3}H-DZN reagent and the subsequent photolysis step do not perturb protein structure. This is indeed the case, as shown by the invariance of the near and far UV CD spectra (Figure 1A and 1B) that are sensitive probes of changes in the tertiary and secondary structure, respectively (*42*).

After the photolysis step, to reach a reliable estimate of the extent of protein labeling, one should be able to accurately measure the fraction of the reagent that becomes covalently attached to the polypeptide chain. To achieve this goal, one has to ensure the efficient removal of any trace of byproducts. Routinely, the workup procedure developed for this purpose consists of (i) an unfolding step in 8 M urea, followed by (ii) dialysis and (iii) RP-HPLC chromatography. In a typical elution profile of a labeled protein sample (Figure 1C), a radioactivity peak is always associated to the mass (absorption) peak. This demonstrates unambiguously the covalent incorporation of ^{3}H-methylene carbene to the protein. Nevertheless, the eluted radioactivity shows a small increase in the retention time and is somewhat broadened with respect to the mass peak. Both facts point to the slightly more hydrophobic nature of the product and the intrinsic chemical heterogeneity brought about by the methylation reaction. At the very low level of methylene incorporation achieved under these experimental conditions, the slight broadening of the elution peak arises from a collection of microscopic molecular species where a single methylene group is expected to be attached to different sites along the polypeptide chain. This contention is fully consistent with the known unspecificity of the reaction, a characteristic of the extreme reactivity of the methylene carbene. In addition, (i) no modification occurs in the absence of photoirradiation, and (ii) negligible incorporation of radioactive label takes place in a control sample where a ^{3}H-DZN solution was first photolyzed and thereafter mixed with BL-βL (data not shown). This allowed us to discard any contribution of 'dark reactions' to the labeled product.

On the other hand, the specific radioactivity incorporated into the protein shows a linear dependence on the concentration of ^{3}H-DZN (Figure 1D). Interestingly, the slope of the graph (8.3×10^{-3} mol CH_2/mol protein/mM DZN) becomes identical to that measured before for bovine α-lactalbumin (α-LA: $3.7 \cdot 10^{-3}$ mol CH_2/mol protein/mM DZN: 20), once these values are normalized by the ASA of each protein. This behavior is consistent with the unspecific character of the photoreaction with target sites in the protein, regardless of their chemical nature.

A main advantage of the application of the methylene labeling technique to study conformational transitions in proteins or protein−protein interactions is that the methylation reaction is not influenced by the solvent environment, as attested by the invariance in the extent of modification of the polypeptide chain dissolved in buffers of different chemical nature, denaturants, or various pH conditions. To support this statement, under experimental conditions where no conformational changes occur, no differences in the yield of methylene labeling were ever observed. These are the cases of hen egg white lysozyme (HEWL) at neutral pH in phosphates buffer (*22*) or in the pH range 2−7 in AGT buffers (*43*), α-LA in the urea concentration range 0.2−4.0 M (*20*), and BL-βL at high urea concentration (~7.0 M) (this work, Figure 2). However, in the last two cases a conformation-independent effect of urea (at mM concentration) or pH indeed exists and likely represents their influence on DZN binding sites present in the native state, as will be discussed below.

Conformational Transitions of BL-βL Followed by ^{3}H-Methylene Labeling. The N−U Transition. ^{3}H-Methylene labeling of BL-βL as a function of urea concentration shows that this experimental parameter is able to distinguish between native (N) and unfolded (U) states of this protein, as attested by the fact that the unfolded state in 7 M urea is labeled 60% more than the native state (Figure 2). Moreover, one can appreciate the ability of this technique to follow more subtle changes along the conformational transition.

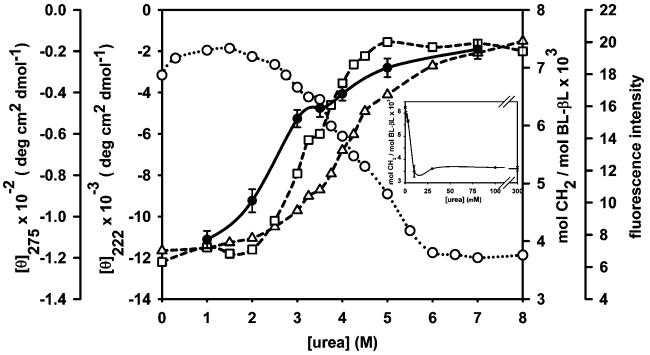

FIGURE 2: Labeling of BL-βL with ^{3}H-methylene as a function of urea concentration. BL-βL samples (30 μM) dissolved in 20 mM sodium phosphate buffer, pH 7.4, and ^{3}H-DZN were photolyzed for 45 min in the presence of different urea concentrations (0−7 M). The extent of methylene carbene incorporation into the protein sample was expressed as the average number of moles of CH_2 per mole of protein normalized at 1 mM ^{3}H-DZN (solid circles and continuous line). The conformational transition was also monitored by changes in the molar ellipticity at 222 nm (open triangles and dashed line) and 275 nm (open squares and dashed line) and in the intrinsic fluorescence (open circles and dotted line). The inset shows the dependence of ^{3}H-methylene labeling at low urea concentrations.

To prove the validity of this approach, parallel measurements of CD (in both UV regions) and the intensity of the intrinsic tryptophan fluorescence were carried out for the sake of comparison. The diversity in the traces of the unfolding curves monitored by the spectroscopic techniques clearly supports the existence of intermediates, as was also observed by others in this same protein system (*25*, *44*−46) and in a related βL of *S. aureus* (*47*). An added dimension in this complex transition is here provided by the methylene labeling data. The presence of at least three states was inferred from two sequential transitions occurring at 1.5−3.0 M and 3.5−6.5 M urea, involving a partially unfolded state I (predominant between 3.0 and 3.5 M urea). Interestingly, in the first transition (N−I) ^{3}H-DZN labeling shows the largest amplitude: 67% of the total change observed, as compared to the magnitude of changes in the CD signals: 56% for $[\theta]_{275}$ and 29% for $[\theta]_{222}$. Even at the highest urea concentration assayed (8 M), 18% of the far UV−CD signal remains, indicating the presence of residual secondary structure in the U state. In addition, a relatively minor perturbation in the environment of tryptophan would occur in state I, as judged by the small amplitude of the change in the fluorescence intensity (24% of the total change is observed in the first transition) and the invariance of the maximum of the spectra (∼337 nm) in the range 0−3.5 M urea. By contrast, both parameters change dramatically as the protein proceeds from state I to state U (the maximum shifts to ∼351 nm in the latter).

Remarkably, apart from the substantial increase in the extent of labeling with ^{3}H-methylene occurring upon unfolding, a smaller but significant *decrease* is observed at very low urea concentration, in a range where no conformational changes are evident by spectroscopy (inset to Figure 2). One likely explanation for this phenomenon, which was also reported for α-LA (*20*) and might well represent the general behavior of many proteins, would be the displacement of ^{3}H-DZN by urea from binding sites present in the N state (note that 1−10 mM urea concentration is comparable to the concentration of ^{3}H-DZN in the samples).

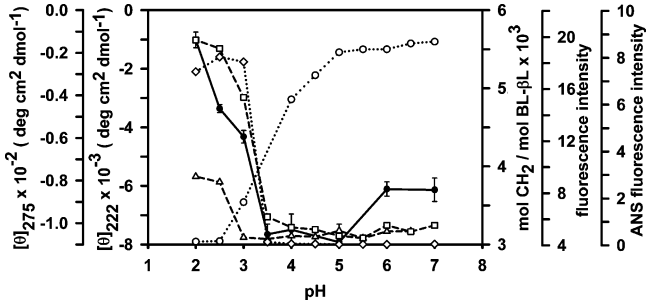

FIGURE 3: Labeling of BL-βL with ^{3}H-methylene as a function of pH. BL-βL samples (30 μM) dissolved in 90 mM AGT buffer at the indicated pH and ^{3}H-DZN were photolyzed for 45 min. The extent of methylene carbene incorporation into the protein sample was expressed as the average number of moles of CH_2 per mole of protein normalized at 1 mM ^{3}H-DZN (solid circles and continuous line). The conformational transition was also monitored by changes in the molar ellipticity at 222 nm (open triangles and dashed line) and 275 nm (open squares and dashed line) and in the intrinsic fluorescence (open circles and dotted line) or ANS fluorescence (open diamonds and dotted line).

The N−A Transition. The solvent environment around the protein determines the appearance and stabilization of partially folded states. In the case of BL-βL, an acidic milieu (pH 2) permits the isolation of a molten globule-like state, the so-called state A (*44*). ^{3}H-methylene labeling of BL-βL as a function of pH demonstrates the ability of the technique to differentiate between N and A states. Proof of this is the fact that the latter is labeled 70% more than the former (Figure 3). Likewise, the technique is able to monitor changes along this conformational transition, including complexities associated to possible substates populated below pH 3.5.

Here again, to contrast results derived from ^{3}H-DZN labeling, parallel spectroscopic measurements were carried out in the range of pH between 2 and 7: far and near UV CD, intrinsic tryptophan fluorescence, and fluorescence of the extrinsic probe ANS. Remarkably, ^{3}H-methylene labeling follows a pattern similar to those probes of tertiary structure, i.e., at pH ≤ 3.5 $[\theta]_{275}$ becomes negligible, and fluorescence emission from ANS at 477 nm shows a pronounced increment as a consequence of binding of this molecule to the protein. Intrinsic tryptophan fluorescence exhibits a major decrease in intensity in the same pH range (although it starts to change at pH ≤ 5.0). In a parallel fashion, a shift in the maximum of emission also occurs: from 337 nm in samples equilibrated at pH 4−7 to 340 nm at pH 2.0 (spectra not shown). This fact suggests a somewhat higher exposure of W residues to the aqueous solvent in state A but far from the value measured for the U state (see above). Finally, we observed a decrease of only 28% in the absolute value of $[\theta]_{222}$ at pH ≤ 3. Taken all this evidence together, state A gathers features that resemble closely those described before for state I. Both behave in a manner fully consistent with the paradigm for the molten globule state: absence of defined tertiary interactions, preservation of substantial secondary structure content, and permeation to the aqueous solvent (*48*).

In the course of these experiments, a *decrease* of lesser magnitude in the extent of labeling was observed in samples equilibrated at pH 5 as compared to those at pH 7, well within a range where no conformational changes occur. This phenomenon bears resemblance to that observed at very low urea concentrations (see above) and might result as a consequence of the displacement of the reagent from binding

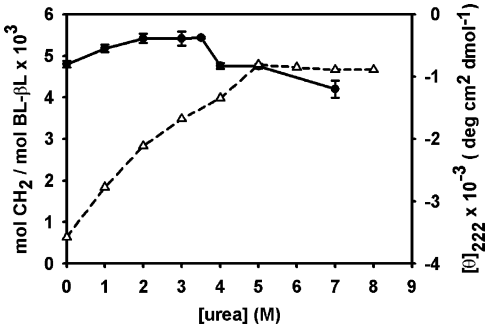

FIGURE 4: Labeling of BL-βL with ^{3}H-methylene at pH 2.0 as a function of urea concentration. BL-βL samples (30 μM) dissolved in 90 mM AGT buffer, pH 2.0, and ^{3}H-DZN were photolyzed for 45 min in the presence of different urea concentrations (0−7 M). The extent of methylene carbene incorporation into the protein sample was expressed as the average number of moles of CH_2 per mole of protein normalized at 1 mM ^{3}H-DZN (solid circles and continuous line). The conformational transition was also monitored by changes in the molar ellipticity at 222 nm (open triangles and dashed line).

sites present in the N state. Tentatively, here protonation of critical amino acid side chains might bring about this effect.

The A−U Transition. BL-βL was labeled with ^{3}H-DZN at pH 2 as a function of urea concentration, with the aim of checking the internal consistency of results so far obtained along the N−U and N−A transitions: i.e. the ~60% and ~70% increases in the extent of labeling for the former and latter, respectively. In this fashion, the A state will turn into the U state, and a minor decrease in the extent of labeling would be expected. Indeed, a 12% decrease in this parameter was observed (Figure 4). This data allows one to compare two conformational states of different nature but predictably sharing a larger solvent-accessible surface area than the N state (see Discussion).

In this case, the appropriate spectroscopic probe to monitor this transition is the absolute value of $[\theta]_{222}$, a parameter showing a monotonous decrement in the signal up to 5 M urea as a consequence of the loss of ordered secondary structure. This describes a non-cooperative behavior not uncommon for other proteins (*49*, *50*). Even at the highest urea concentration assayed, residual order in the polypeptide chain persists at this acidic pH, in a fashion similar to the observation in the N−U transition (see above).

Peptide Analysis of BL-βL Labeled in the Native and Unfolded States. To identify sites labeled with ^{3}H-methylene along the polypeptide chain, we measured the radioactivity associated to peptides derived from CNBr cleavage of BL-βL samples modified under native or denaturing conditions. This methodology allowed us to obtain a limited number of fragments of BL-βL that map to different subdomains of the protein (BL-βL includes five Met residues), thus facilitating data interpretation. It is noteworthy that the strong acidic conditions necessary for CNBr cleavage are compatible with the preservation of the methylene addition, i.e., no appreciable loss of label occurs (data not shown). The peptide mixture produced after the cleavage reaction was separated by RP-HPLC on a C4 column, and the collected fragments were subsequently identified by amino acid analysis and peptide sequencing (Figure 5 and Table 1). Taken together, the isolated peptides represent a continuous stretch covering 95% of the total amino acid sequence of BL-βL (the remainder corresponds to the unstructured N- and C-termini).

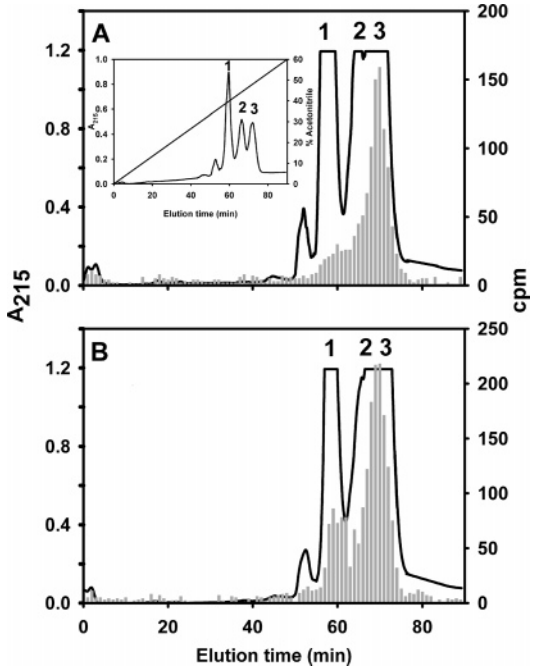

FIGURE 5: Separation by RP-HPLC of CNBr peptides derived from BL-βL photolabeled with ^{3}H-methylene. Samples of BL-βL under native (A) or denaturing conditions (B: in the presence of 8 M urea) were photolabeled, cleaned-up, and cleaved with CNBr. The resulting peptides were separated on a C4 column, and the elution was monitored by both UV absorption at 215 nm (solid line) and by the measurement of the radioactivity associated to each collected fraction (gray bars). Less amount of the peptide mixture was sampled onto the same column and run under identical chromatographic conditions to show that effective separation of all three peptides is achieved in all cases (inset). Isocratic elution with 0.05% aqueous TFA (20 min) was followed by a linear gradient (straight line) of acetonitrile:water (0 to 60% in 90 min) in 0.05% TFA at a 3.0 mL/min flow rate. Peak numbers correspond to the peptides listed in Table 1.

Table 1: CNBr Peptides of BLβL Separated by RP-HPLC

peptide	amino acid position[a]	U/N labeling ratio[b]	U/N ASA ratio[c] extended/N	max/N	min/N
1	212−287	1.86	3.61	3.81	2.95
2	118−211	0.87	3.88	3.84	2.98
3	30−117	1.56	2.86	3.07	2.37

[a] Unambiguous identification of each peptide isolated by RP-HPLC (see Figure 5) was achieved by Edman microsequencing and ES-MS. [b] The U/N labeling ratio is calculated as the extent of ^{3}H-methylene labeling (as estimated by the radioactivity present under each peak) of a sample modified under denaturing conditions (U) relative to an identical amount of sample modified in the native state (N). [c] The U/N ASA ratio is the quotient between the ASA of each peptide in the unfolded (U) and native (N) states. ASA N was calculated from the crystallographic structure of BL-βL (pdb code 4blm) and ASA U from different theoretical models of the unfolded state: extended, max, and min, as described in Experimental Procedures.

Key to this analysis is to perform a careful comparison of the incorporated radioactivity along the chromatographic profile in peptides derived from BL-βL labeled in a given conformational state. To this end, very similar amounts of peptide mixtures were sampled. Here we noticed the following general features of the RP-HPLC separation. (i) All radioactivity was observed between the boundaries of elution of the peptides and in close association with any given fraction, as expected for a general labeling phenomenon that

causes minimal modification of the polypeptide chain. (ii) A trend exists to have more methylene label incorporation as the molecular mass and/or the hydrophobicity of the peptides increase, a fact that agrees with the indiscriminate reactivity of the methylene carbene. (iii) Overall, an increment of 65% in label incorporation was observed for the U state relative to the N state. This value agrees well with the increment measured for the whole protein (see above data for the N−U transition). (iv) Similarly, a cross comparison was carried out *for each isolated peptide*, where results are expressed as U/N labeling ratios (Table 1). The individual behavior of each peptide is not uniform. Although the general trend points to an increase in labeling, yielding U/N ratios higher than one, as observed for peptides 1 and 3, a different result is observed for peptide 2. Further enzymatic digestion with trypsin and separation by size exclusion chromatography of all three peptides rendered profiles from which confirmatory evidence was derived. Thus, peptide 1 and 3 produced patterns where the U/N ratio is consistently higher than one for all tryptic peptides, whereas peptide 2 exhibited a clear 'inversion' of the ratio at certain fractions (e.g., U/N ratios as low as 0.37, data not shown).

The observation of differences in the extent of labeling along the polypeptide chain, rather than being a peculiar aspect of BL-βL, is common to other proteins, as was demonstrated for α-LA (*20*) and HEWL (*22*). The main source of these differences does not arise from the intrinsic chemical nature of the target functional groups, but rather from the conformational state of the peptide, which will obviously affect the microenvironment around a given site. The overall increment in labeling and the individual values measured for each peptide are most relevant pieces of information that will be discussed later in terms of the increased surface exposure predicted at different sites along the polypeptide chain.

DISCUSSION

Methylene Carbene as an Unspecific and Nonintrusive Probe of the Polypeptide Surface. In order to attempt any chemical modification experiment aimed at addressing conformational aspects of the protein, one should ensure that the reagent itself does not pose a structural perturbation on the system. This is indeed the case, as shown in Figure 1A and 1B, where it becomes evident that neither the codissolution of the parent reagent DZN in the protein sample nor the ensuing photoirradiation step necessary to cause insertion of the methylene biradical affect conformation. Nevertheless, one should bear in mind that at the typical extents of modification achievable under our experimental conditions only a minor fraction of the protein molecules in the sample will become methylated.

This work underscores the novel applicability of this reaction to modify the polypeptide chain immersed in its natural aqueous environment and relates this to the concept of accessible surface area (ASA). Because ASA is expected to depend strongly on the folding state of the protein, one would predict the realization of an experimental measurement of this critical parameter through DZN labeling.

The linearity observed in Figure 1D is consistent with a collisional behavior for the reaction of methylene carbene with the protein, where no appreciable affinity of DZN needs to be invoked, i.e., under our experimental conditions no hint of curvature suggesting a hyperbolic behavior is seen. Indeed, typically the 'binding affinities' measured for small organic molecules to proteins (HEWL) range between 0.1 and 5 M^{-1} (*51*). In support of the collisional behavior, a simple theoretical analysis that considers the mole fraction (R) of the ASA of the protein with respect to all components present in the system (that includes the buffer and the water solvent) yields a reasonably good estimate of the experimentally determined extent of protein modification, as is discussed next. The *R* value equals the ratio of the following products: (i) the ASA of BL-βL (12 576 $Å^2$, estimated from pdb file 4blm, using a probe radius of 1.4 Å) times the concentration of this protein in the sample (25 μM), and (ii) the total ASA available for labeling in the system, i.e., the sum of the corresponding products calculated for the protein, the buffer, and the water solvent (essentially dominated by that for the latter: 32.4 $Å^2$ times 55.55 M). If the incorporation of label follows a purely unspecific mode, that is, if the reagent adds to components of the system proportionally to the available area, then one would expect a fraction *R* of methylene equal to 0.175‰ incorporated into the protein component, that is an amount equivalent to 7×10^{-3} mol of methylene per mole of protein, at a standard concentration of 1 mM bulk ^{3}H-DZN reagent. Indeed, the experimentally determined slope of 8.3×10^{-3} mol CH_2/mol protein/mM DZN (Figure 1D) agrees very well with the prediction. An identical calculation carried out for α-LA (ASA: 7236 $Å^2$, taken from pdb file 1hfz, subunit D) yields a value of 4×10^{-3} mol CH_2/mol protein/mM DZN, that is also in excelent agreement with experiment: 4.1×10^{-3} mol CH_2/mol protein/mM DZN (*20*). Taking these values together, one can estimate that, on average, $\sim 6 \times 10^{-7}$ molecules CH_2 per $Å^2$ at 1 mM DZN will be incorporated. Related to this point, an independent study aimed at measuring the ASA occluded due to an antigen−antibody interaction between HEWL and the immunoglobulin IgG_1D1.3 (749 $Å^2$, measured in pdb file 1vfb) yielded a value of 0.44×10^{-3} mol CH_2/mol protein/mM DZN for the difference in the labeling extent between free and complexed HEWL (*22*). The ratio between these numbers equals 5.9×10^{-7} molecules CH_2 per $Å^2$ at 1 mM DZN, a value remarkably close to that reported above.

Nevertheless, one should point out that this correlation found between different proteins in their native states necessarily includes features of their surface that might influence the final experimental value observed. For instance, the presence of cavities or crevices or hydrophobic patches, with areas of different sizes that might favor DZN partition, would tend to overestimate the measurements, as will be discussed below. In principle, one would expect a more straightforward correlation for the unfolded state because the latter will lack the topographical complexities associated with more structured conformations.

^{3}H-Methylene Labeling Is Sensitive to the Conformational State of the Protein. The cross comparison between the profile of methylene labeling and measurements derived from other biophysical methods such as CD and fluorescence demonstrates a close correlation with those probes most sensitive to changes in tertiary structure. This contention is supported by the observations that (i) along the urea-induced N−I−U transition (Figure 2) the most significant change in

DZN labeling occurs along the N−I portion, and (ii) along the acid pH-induced N−A transition (Figure 3) DZN labeling shows a large amplitude change in parallel with optical probes of tertiary structure (Trp fluorescence, ANS binding, and near UV CD).

Careful comparison of the extent of labeling corresponding to each state assayed allowed us to attempt inferences on the *extent* and *nature* of the surface exposed to the aqueous solvent. We hypothesize that the close packing characteristic of the native state would represent the main impediment to the penetration of the DZN probe, in a fashion similar to that experienced by the water solvent. On the other hand, ready accessibility to the solvent governs the behavior of the unfolded state, where an increase in DZN labeling is the common observation. In between these extremes, one finds the I (or A) states, where the increment observed with respect to the native state is consistent with (i) the proposed loosening of tight interactions in the core of the protein allowing enhanced permeation of solvent and probe, and (ii) the concomitant appearance of a hydrophobic 'phase' prone to a more favorable partition of the reagent. The organization of this putative hydrophobic phase would no longer persist in the unfolded state.

From a quantitative elaboration on the extent of labeling observed for each conformational state alongside theoretical estimates of the ASA parameter one can draw useful insights on features of the native and non-native states. In regard to this point, a ∼60% increment in the extent of methylene labeling was observed along the urea-induced N−U transition. An interpretation of this result requires taking into account the geometry expected for the unfolded state. Because there is no consensus picture on the nature of the latter, one should compare experimental measurements with accurate predictions derived from different models: (i) an extended chain (phi and psi 180°) marks the upper limit of solvent exposure for the polypeptide (ASAextended); (ii) alternatively, one can regard a statistical ensemble of fluctuating conformers simulated with a Monte Carlo technique and a hard sphere potential (ASAmax, *38*, *39*); (iii) the surface of the fragments folded as in the native state renders the lower bound (ASAmin, *38*, *39*). The consideration of a fully extended chain predicts an increment that lies way above that observed (∼190−195%). Under the assumptions described before for ASAmax and ASAmin, the corresponding increments in solvent accessibility would be ∼199% and ∼132%, respectively. Even under the most realistic model considered here (ASAmin), predictions still overestimate solvent exposure. Nevertheless, thermodynamic considerations on the unfolding process based on calorimetry put forward the notion that the unfolded state would expose at most about two-thirds of the value calculated for the fully extended chain model (*52*). Taking into account this result, an upper boundary of ∼97% would be set to the increment in ASA associated to the BL-βL unfolding. In addition, a residual dichroic signal exists in the presence of 8 M urea (∼18% of that measured at 222 nm for the native state). Taken together, this evidence would point to the fact that the unfolded state would differ significantly from a purely extended form. This is fully consistent with the notion that in many cases a certain extent of remaining structure persists in the unfolded state (*53*, *54*). At the other end, the presence of cavities and crevices known to exist in the native state might cause the binding of DZN, thus incrementing the residence time of the reagent at certain sites (see below) and consequently augmenting the extent of methylene labeling. The combined effect of these factors will bring about a reduction in the increment of labeling expected in progressing from the native to the unfolded state.

A different effect, albeit of lesser magnitude, is also observed at very low concentration of the denaturant (inset to Figure 2). Here, no change in conformation due to weakening of hydrophobic interactions should be invoked, but rather a urea-borne 'uncoating' of the protein surface from sites putatively occupied by DZN. This is consistent with (i) the existence of hydrophobic spots on the surface and/or cavities, where the reagent would be expected to reside longer, and (ii) the micromolar affinity measured for urea binding to protein surfaces as opposed to the millimolar to molar affinities expected for gases of similar size to DZN (see above), thus presumably causing the ready displacement of the latter by the former.

The extreme reactivity of the methylene carbene species offers a technical advantage over other conventional chemical modification reagents, bringing about the possibility of reacting with the polypeptide chain regardless of the pH of the milieu. Proof of the latter is the invariance in the extent of modification that has been demonstrated for HEWL in the pH range 2−7, where its native conformation is preserved (*43*). Unlike the former behavior, for BL-βL an increment of 70% in methylene labeling is observed for the A state with respect to the N state (Figure 3). This marks a sharp transition that runs in parallel with optical measurements and, in particular, with the binding of the fluorescent dye ANS. This probe is believed to bind to clusters of nonpolar atoms accessible to the solvent that are absent in the denatured state and are relatively rare in the native state (*55*). In this fashion, the intermediate A is consistent with a state exhibiting exposed (hydrophobic) patches, substantially altered tertiary interactions and only a minor loss of secondary structure. All these features characterize a molten globule state for BL-βL, as it has been described by others (*28*, *47*, *56*, *57*). The emerging picture for state A includes the conservation of a hydrophobic, although less well-packed core, exhibiting a more ready accessibility to the aqueous solvent and likewise to the reagent.

Finally, the extent of methylene labeling decreases minimally (∼12%) along the non-cooperative A−U transition (Figure 4). This fact might arise as the consequence of a balance between the following phenomena: (i) the preferential partition of the reagent DZN in hydrophobic regions present in the A state; (ii) the expected ASA increase occurring upon protein unfolding. This emphasizes the above-mentioned usefulness of DZN labeling to monitor changes of tertiary structure and, less so, of secondary structure, as demonstrated by the gradual and large amplitude change of secondary structure content (as shown by $[\theta]_{222}$). Here, it is noteworthy to state that there hardly exists much difference in the extent of solvent exposure between the polypeptide chain adopting a random or extended conformation and one folded as an α helix (result not shown). This arises mostly from the much larger weight of the side chains of amino acids on the total surface of the polypeptide.

Methylene Carbene Labeling Reveals Local Features of the Folding of BL-βL. A thorough peptide analysis of those

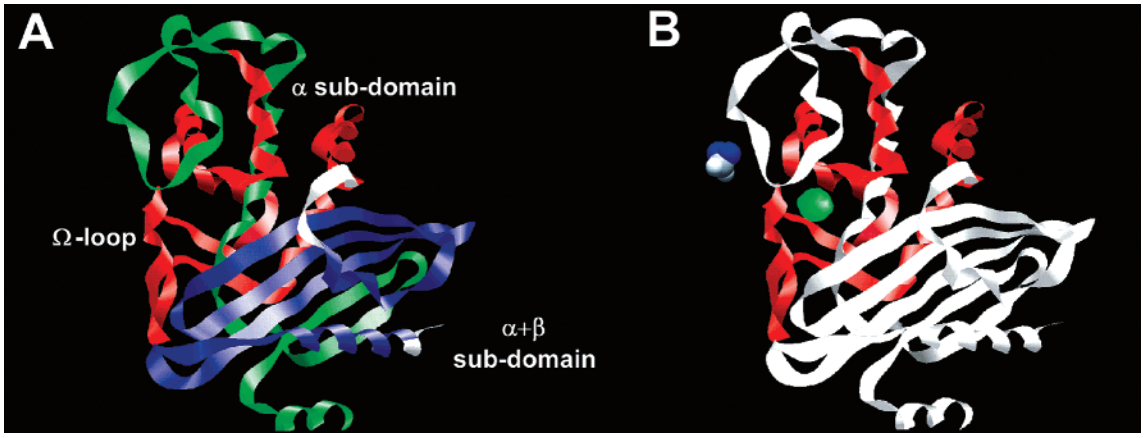

FIGURE 6: Structure of native BL-βL (pdb code 4blm: *27*). (A) Peptides 1−3 (see Table 1) are colored in blue, red, and green, respectively. (B) The peptide having an anomalously low labeling increment (peptide 2) is colored in red, and the remainder of the protein is shown in white. The major cavity (64 Å^3), delimited by residues Q135, L139, P145, L148, P162, R164, L169, and D179, is illustrated as a blob colored in green. For the sake of comparison, a DZN molecule is shown as a CPK model (43 Å^3). Cavity volumes and boundaries were calculated with MSP (*40*) using a probe radius of 1.4 Å. The final figure was rendered with GRASP (*41*).

extreme cases represented by the N and U states allowed us to produce a map of local solvent accessibility (Figures 5 and 6). On average, in the U state, peptide labeling amounts to 6.95 cpm/mol amino acid residue, whereas in the N state, this value is 4.20 cpm/mol amino acid residue. Therefore, an increment of 65% is observed for the former relative to the latter, a result fully consistent with measurements obtained for the whole protein (cf. 60% for the N−U transition, see above). In addition, as has also been observed for α-LA (*20*), the variation in the extent of labeling among different peptides is greater in the N state than in the U state, an observation pointing to the lesser influence exerted by the environment on the yield of reaction in the latter case.

The U/N labeling ratio measured for each isolated peptide provides a reliable experimental estimate that can best be correlated with conformational aspects (Figure 6 and Table 1). Given the shortcomings implied in each model for the unfolded state, one should not expect to find a straightforward correspondence in the absolute values. All these predictions tend to overestimate the solvent exposure of the unfolded state. However, a positive correlation in relative terms could be traced, and that would include the cases of peptides 1 and 3, where the experimental U/N ratio matches the more realistic min/N theoretical estimate. This was also the case for a larger set of tryptic peptides derived from α-LA (*20*). At variance with this, peptide 2 is a clear outlier: here the U/N is inverted. To address this point, a detailed description of the *native state* should offer a hint on this behavior. The BL-βL structure can be envisioned as a close association between two subdomains: one characterized by an α+β motif and the other rich in α structure. Two crevices lie at the interface between these subdomains, one of which forms the active site cleft (*26*, *27*, *58*, *59*). This constitutes a poorly packed region where water molecules occur and possibly exhibiting enhanced flexibility. In addition, the largest cavity occurs in this neighborhood: it shows an irregular shape and is bounded by helix α2, the so-called Ω-loop and residues pertaining to helices α5 and α6. In this regard, the presence of crevices or cavities that could potentially lodge the reagent DZN −thus favoring its partition into these sites- would present a preferential target for labeling in state N. It is suggestive that the 'anomalously' labeled peptide 2 actually includes all the amino acids belonging to the Ω-loop and those lining the major cavity in BL-βL (of 64 Å^3 and limited by Q135, L139, P145, L148, P162, R164, L169, and D179, see Figure 6B). This space is big enough to fit DZN (∼43−45 Å^3), provided that water molecules could be expelled from the site.

CONCLUSIONS AND PERSPECTIVES

In this work we demonstrate the general usefulness of a novel technique based on the photochemically triggered methylene labeling of the polypeptide chain to follow conformational transitions in proteins. This is exemplified here by BL-βL, a protein undergoing defined changes in its conformation as a consequence of modification of the solvent environment. In particular, methylene labeling made possible a comparative structural characterization of the native as well as non-native states, including partially folded (molten globule) and unfolded ensembles. The accurate determination of the extent of labeling enlightens even subtle aspects of complex transitions and introduces an original (and perhaps unique) experimental measurement of ASA. The improved resolution of this analysis at the level of peptides provides profiles of solvent accessibility along the amino acid sequence from which three-dimensional information can be derived. Further developments along these lines would permit study of short-lived kinetic intermediates through the use of very powerful (synchrotron) light sources for the photolysis step. At the analytical front, modern mass spectrometry methods will be used with advantage to detect the excess mass associated to the methylated products, thus avoiding the use of radiotracers.

ACKNOWLEDGMENT

We thank Dr. Javier Santos for his helpful comments and critical reading of the manuscript.

REFERENCES

1. Dill, K. A., and Shortle, D. (1991) Denatured states of proteins, *Annu. Rev. Biochem. 60*, 795−825.
2. Ptitsyn, O. B. (1995) Molten globule and protein folding, *Adv. Protein Chem. 47*, 83−229.
3. Arai, M., and Kuwajima, K. (2000) Role of the molten globule state in protein folding, *Adv. Protein Chem.* 53, 209−282.

4. Hammes, G. G. (2005) *Spectroscopy for the biological sciences*, John Wiley & Sons, Inc., Hoboken, NJ.
5. Fersht, A. (1999) *Structure and mechanism in protein science: a guide to enzyme catalysis and protein folding*, W. H. Freeman and Company, New York, NY.
6. Creighton, T. E., ed. (1992) *Protein folding*, W. H. Freeman and Company, New York, NY.
7. Pain, R. H., ed. (1994) *Mechanisms of protein folding*, IRL Press at Oxford University Press, Oxford, U. K.
8. Lee, B., and Richards, F. M. (1971) The interpretation of protein structures: estimation of static accessibility, *J. Mol. Biol. 55*, 379−400.
9. Miller, S., Janin, J., Lesk, A. M., and Chothia, C. (1987) Interior and surface of monomeric proteins, *J. Mol. Biol. 196*, 641−656.
10. Pace, C. N. (2001) Polar group burial contributes more to protein stability than nonpolar group burial, *Biochemistry 40*, 310−313.
11. Lundblad, R. L. (2005) *Chemical reagents for protein modification*, 3rd ed., CRC Press, Boca Raton, FL.
12. Goshe, M. B., and Anderson, V. E. (1999) Hydroxyl radical-induced hydrogen/deuterium exchange in amino acid carbon-hydrogen bonds, *Radiat. Res. 151*, 50−58.
13. Goshe, M. B., Chen, Y. H., and Anderson, V. E. (2000) Identification of the sites of hydroxyl radical reaction with peptides by hydrogen/deuterium exchange: prevalence of reactions with the side chains, *Biochemistry 39*, 1761−1770.
14. Maleknia, S. D., Brenowitz, M., and Chance, M. R. (1999) Millisecond radiolytic modification of peptides by synchrotron X-rays identified by mass spectrometry, *Anal. Chem. 71*, 3965−3973.
15. Maleknia, S. D., Ralston, C. Y., Brenowitz, M. D., Downard, K. M., and Chance, M. R. (2001) Determination of macromolecular folding and structure by synchrotron x-ray radiolysis techniques, *Anal. Biochem. 289*, 103−115.
16. Maleknia, S. D., and Downard, K. M. (2001) Unfolding of apomyoglobin helices by synchrotron radiolysis and mass spectrometry, *Eur. J. Biochem. 268*, 5578−5588.
17. Englander, S. W., and Krishna, M. M. G. (2001) Hydrogen exchange, *Nat. Struct. Biol. 8*, 741−742.
18. Nukuna, B. N., Goshe, M. B., and Anderson, V. E. (2001) Sites of hydroxyl radical reaction with amino acids identified by (2)H NMR detection of induced (1)H/(2)H exchange, *J. Am. Chem. Soc. 123*, 1208−1214.
19. Richards, F. M., Lamed, R., Wynn, R., Patel, D., and Olack, G. (2000) Methylene as a possible universal footprinting reagent that will include hydrophobic surface areas: overview and feasibility: properties of diazirine as a precursor, *Protein Sci. 9*, 2506−2517.
20. Craig, P. O., Ureta, D. B., and Delfino, J. M. (2002) Probing protein conformation with a minimal photochemical reagent, *Protein Sci. 11*, 1353−1366.
21. Nuss, J. E., and Alter, G. M. (2004) Denaturation of replication protein A reveals an alternative conformation with intact domain structure and oligonucleotide binding activity, *Protein Sci. 13*, 1365−1378.
22. Gómez, G. E., Cauerhff, A., Craig, P. O., Goldbaum, F. A., and Delfino, J. M. (2006) Exploring protein interfaces with a general photochemical reagent, *Protein Sci. 15*, 744−752.
23. Delfino, J. M., Schreiber, S. L., and Richards, F. M. (1993) Design, synthesis and properties of a photoactivatable membrane-spanning phospholipidic probe, *J. Am. Chem. Soc. 115*, 3458−3474.
24. Weber, T., and Brunner, J. (1995) 2-(Tributylstannyl)-4-[3-(trifluoromethyl)-3H-diazirin-3-yl]benzyl Alcohol: A Building Block for Photolabeling and Cross-Linking Reagents of Very High Specific Radioactivity, *J. Am. Chem. Soc. 117*, 3084−3095.
25. Frate, M. C., Lietz, E. J., Santos, J., Rossi, J. P., Fink, A. L., and Ermacora, M. R. (2000) Export and folding of signal-sequenceless Bacillus licheniformis beta-lactamase in Escherichia coli, *Eur. J. Biochem. 267*, 3836−3847.
26. Moews, P. C., Knox, J. R., Dideberg, O., Charlier, P., and Frere, J. M. (1990) Beta-lactamase of Bacillus licheniformis 749/C at 2 Å resolution. *Proteins 7*, 156−171.
27. Knox, J. R., and Moews, P. C. (1991) Beta-lactamase of Bacillus licheniformis 749/C. Refinement at 2 Å resolution and analysis of hydration, *J. Mol. Biol. 220*, 435−455.
28. Goto, Y., Calciano, L. J., and Fink, A. L. (1990) Acid-induced folding of proteins, *Proc. Natl. Acad. Sci. U. S. A. 87*, 573−577.
29. Yanagida, N., Uozumi, T., and Beppu, T. (1986) Specific excretion of Serratia marcescens protease through the outer membrane of Escherichia coli, *J. Bacteriol. 166*, 937−944.
30. Jansson, J. A. (1965) A Direct Spectrophotometric Assay For Penicillin Beta-Lactamase (Penicillinase), *Biochim. Biophys. Acta 99*, 171−172.
31. Schagger, H., and von Jagow, G. (1987) Tricine-sodium dodecyl sulfate-polyacrylamide gel electrophoresis for the separation of proteins in the range from 1 to 100 kDa, *Anal. Biochem. 166*, 368−379.
32. Ellerby, L. M., Escobar, W. A., Fink, A. L., Mitchinson, C., and Wells, J. A. (1990) The role of lysine-234 in b-lactamase catalysis probed by site-directed mutagenesis, *Biochemistry 29*, 5797−5806.
33. Kamp, R. M. (1986) in *Advanced Methods in Protein Microsequence Analysis*, pp 8−20, Springer-Verlag, Berlin.
34. Fontana, A., and Gross, E. (1987) Fragmentation of polypeptides by chemical methods, in *Practical Protein Chemistry-a Handbook*, pp 67−120, John Wiley & Sons Ltd, New York NY.
35. Wilkinson, J. M. (1986) in *Practical Protein Chemistry-A Handbook*, pp 121−148. John Wiley & Sons Ltd., Chichester.
36. Edman, P., and Begg, G. (1967) A protein sequenator, *Eur. J. Biochem. 1*, 80−91.
37. Mohamadi, F., Richards, N. G. J., Guida, W. C., Liskamp, R., Lipton, M., Caufield, C., Chang, G., Hendrickson, T., and Still, W. C. (1990) Macromodel-An integrated software system for modeling organic and bioorganic molecules using molecular mechanics, *J. Comput. Chem. 11*, 440−467.
38. Creamer, T. P., Srinivasan, R., and Rose, G. D. (1995) Modeling unfolded states of peptides and proteins, *Biochemistry 34*, 16245−16250.
39. Creamer, T. P., Srinivasan, R., and Rose, G. D. (1997) Modeling unfolded states of proteins and peptides. II. Backbone solvent accessibility, *Biochemistry 36*, 2832−2835.
40. Connolly, M. L. (1993) The molecular surface package, *J. Mol. Graph. 11*, 139−141.
41. Nicholls, A., Sharp, K. A., and Honig, B. (1991) Protein folding and association: insights from the interfacial and thermodynamic properties of hydrocarbons, *Proteins 11*, 281−296.
42. Fasman, G. D. (1996) *Circular dichroism and the conformational analysis of biomolecules*, Plenum Press, New York, NY.
43. Craig, D.B. (2004). *Diazirine: a photoreactive probe for the conformational study of proteins*, Ph.D. Dissertation, University of Buenos Aires.
44. Calciano, L. J., Escobar, W. A., Millhauser, G. L., Miick, S. M., Rubaloff, J., Todd, A. P., and Fink, A. L. (1993) Side-chain mobility of the β-lactamase A state probed by electron spin resonance spectroscopy, *Biochemistry 32*, 5644−5649.
45. Santos, J., Gebhard, L. G., Risso, V. A., Ferreyra, R. G., Rossi, J. P., and Ermácora, M. R. (2004) Folding of an abridged β-lactamase, *Biochemistry 43*, 1715−1723.
46. Santos, J., Risso, V. A., Sica, M. P.and Ermácora, M. R. (2007) Effects of Serine-to-Cysteine Mutations on {beta}-Lactamase Folding, *Biophys. J. 93*, 1707−1718.
47. Uversky, V. N. (1993) Use of fast protein size-exclusion liquid chromatography to study the unfolding of proteins which denature through the molten globule, *Biochemistry 32*, 13288−13298.
48. Ptitsyn, O. B. (1992) in *Protein folding* (Creighton, T. E., Ed.) pp 243−300, W.H. Freeman and Company, New York, NY.
49. Schulman, B. A., Kim, P. S., Dobson, C. M., and Redfield, C. (1997) A residue-specific NMR view of the non-cooperative unfolding of a molten globule, *Nat. Struct. Biol. 4*, 630−634.
50. Wijesinha-Bettoni, R., Dobson, C. M., and Redfield, C. (2001) Comparison of the denaturant-induced unfolding of the bovine and human alpha-lactalbumin molten globules, *J. Mol. Biol.* 312, 261−273.
51. Liepinsh, E., and Otting, G. (1997) Organic solvents identify specific ligand binding sites on protein surfaces, *Nat. Biotechnol. 15*, 264−268.
52. Lee, B. (1991) Isoenthalpic and isoentropic temperatures and the thermodynamics of protein denaturation, *Proc. Natl. Acad. Sci. U.S.A. 88*, 5154−5158.
53. Baldwin, R. L., and Zimm, B. H. (2000) Are denatured proteins ever random coils? *Proc. Natl. Acad. Sci. U. S. A. 97*, 12391−12392.

54. Shortle, D., and Ackerman, M. S. (2001) Persistence of native-like topology in a denatured protein in 8 M urea, *Science 293*, 487−489.
55. Ptitsyn, O. B., Pain, R. H., Semisotnov, G. V., Zerovnik, E., and Razgulyaev, O. I. (1990) Evidence for a molten globule state as a general intermediate in protein folding, *FEBS Lett. 262*, 20−24.
56. Uversky, V. N., Semisotnov, G. V., Pain, R. H., and Ptitsyn, O. B. (1992) 'All-or-none' mechanism of the molten globule unfolding, *FEBS Lett. 314*, 89−92.
57. Vanhove, M., Lejeune, A., Guillaume, G., Virden, R., Pain, R. H., Schmid, F. X., and Frere, J. M. (1998) A collapsed intermediate with nonnative packing of hydrophobic residues in the folding of TEM-1 b-lactamase, *Biochemistry 37*, 1941−1950.
58. Herzberg, O., and Moult, J. (1987) Bacterial resistance to beta-lactam antibiotics: crystal structure of beta-lactamase from Staphylococcus aureus PC1 at 2.5 Å resolution, *Science 236*, 694−701.
59. Banerjee, S., Pieper, U., Kapadia, G., Pannell, L. K., and Herzberg, O. (1998) Role of the omega-loop in the activity, substrate specificity, and structure of class A b-lactamase, *Biochemistry 37*, 3286−3296.

BI7012867